FULL-WIDTH TESTS TO EVALUATE STRUCTURAL INTERACTION

Yuji Arai
Kunio Yamazaki
Japan Automobile Research Institute
Koji Mizuno
Nagoya University
Hidenobu Kubota
Ministry of Land, Infrastructure and Transport
Japan
Paper Number 07-0195

ABSTRACT

This paper discusses the improvement and assessment of structural interaction in SUV-to-car frontal collisions. For this purpose, a series of crash tests using SUVs and small cars was conducted. The results of the SUV-to-small car crash tests indicated that the aggressiveness of SUVs can be reduced by equipping the SUV with a secondary energy absorbing structure (SEAS) or by aligning the height of the SUV's longitudinal members with that of the small car's longitudinal members. The full-width tests, which had been proposed for the assessment of structural interaction, were conducted to detect and assess SEAS reaction force. The test results indicated that SEAS reaction force is detected in the full-width deformable barrier test and also suggested that vertical structural interaction (VSI) will be a useful criterion for assessing SEAS reaction force.

INTRODUCTION

To improve the compatibility of vehicles of different sizes in a frontal crash, it is necessary to improve the structural interaction in front. Accordingly full-width tests have been proposed to measure barrier force distributions for the improvement and assessment of structural interaction [1-3].

In vehicle crash compatibility, the aggressiveness of the SUV is an important subject to be addressed [4]. The longitudinal members of SUVs are inclined to be higher than those of cars, and a vertical mismatch of longitudinal members between an SUV and a car can occur. This vertical mismatch can lead to an override by the SUV, and cause a large intrusion into the upper part of the passenger compartment of the struck car. Therefore, to prevent the override, it is important to improve structural interaction in the vertical direction. For such improvements, two means are conceivable: a) aligning the height of longitudinal members between car and SUV or b) equipping a SEAS below the longitudinal members of the SUV.

The present study, part of the compatibility research project organized by Japan's Ministry of Land, Infrastructure and Transport, was focused on the structural interaction of SUVs and was intended to examine the vehicle deformation and occupant injury of a small car in a frontal crash with an SUV where the SUV is equipped with a SEAS or the height of the SUV's longitudinal members is aligned with that of the small car's longitudinal members. In addition, full-width rigid barrier test and full-width deformable barrier test were carried out using SUVs with and without SEAS, and the barrier force distributions were examined to detect and evaluate SEAS. Further, repeatability of the full-width deformable barrier test was investigated.

SUV-TO-CAR CRASHES

The SUV-to-small car test was performed in two crash configurations: offset frontal crash and full frontal crash, the latter test conducted by the Japan Automobile Manufacturers Association, Inc. (JAMA). Table 1 shows the test matrix. The impact velocity was 50 km/h with both vehicles traveling. Hybrid III test dummies were used for the front seat driver and passenger positions in each vehicle. The offset frontal crash test was divided into Test 1 and Test 2. In Test 1, the normal SUV with SEAS was used, and in Test 2, the modified SUV with SEAS removed was used. In both Test 1 and Test 2, the overlap ratio was 50% of the small car.

The full frontal crash test was divided into Test 3 and Test 4. In Test 3, the normal SUV with SEAS was used, and in Test 4, the SUV's longitudinal members were located at a lower position aligning with the center height to the small car's longitudinal members. In full frontal crash Test 3, there was a 57 mm vertical gap between normal SUV and small car as measured at the center of the longitudinal member. The overlap ratio was 43% between the longitudinal

members of the two vehicles.

Table 1.
Test matrix of SUV-to-car crash tests

Test configuration	Test vehicle	Impact velocity (km/h)	Test mass (kg)	Overlap ratio (%)	Longitudinal member height difference (mm)
SUV-to-car offset frontal crash (Test 1)	Normal SUV w/ SEAS Small car	50.5	2076 1091	50 (Small car)	63
SUV-to-car offset frontal crash (Test 2)	Modified SUV w/o SEAS Small car	50.1	2076 1091	50 (Small car)	63
SUV-to-car full frontal crash (Test 3)	Normal SUV w/ SEAS Small car	50	2076 1074	100 (Small car)	57
SUV-to-car full frontal crash (Test 4)	Lowered SUV w/ SEAS Small car	50	2076 1074	100 (Small car)	0

Figure 1 shows the front structural components of the normal SUV and small car. The normal SUV is a frame-type vehicle with stiff longitudinal members. The SEAS is mounted directly on the longitudinal members. The distance from the front edge of the bumper cover to the SEAS was 377 mm in a longitudinal direction. The small car has a simple body structure with longitudinal members and bumper beam.

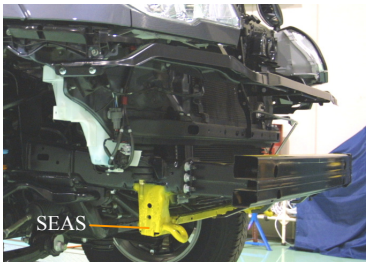

(a) SUV

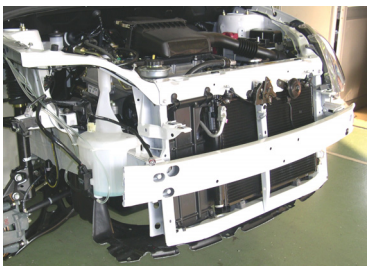

(b) Small car

Figure 1. Front structure of test vehicles.

Offset Frontal Crashes

Figure 2 shows the deformation of the small cars in the SUV-to-car offset frontal crash tests. In the crash tests, geometric misalignments of the longitudinal members existed in the horizontal and vertical directions between SUV and small car. Consequently, the longitudinal member of the SUV impacted the suspension strut and A-pillar of the small car in the two tests. As shown in Figure 3, the SEAS engaged the front wheel of the small car. In contrast, the longitudinal member of the SUV without the SEAS did not engage the front wheel but impacted the A-pillar of the small car. As a result, the A-pillar beltline deformation of the small car in the crash into the SUV without the SEAS was as large as 350 mm, and the small car in the crash into the SUV without the SEAS caused more intrusion at the brake pedal and toe board than the small car in the crash into the SUV with the SEAS (Figure 2).

From the two tests, it was demonstrated that the SEAS of the SUV is quite effective for structural interaction improvement even in a case of lateral mismatch.

(a) Test 1 (vs. normal SUV w/ SEAS)

(b) Test 2 (vs. modified SUV w/o SEAS)

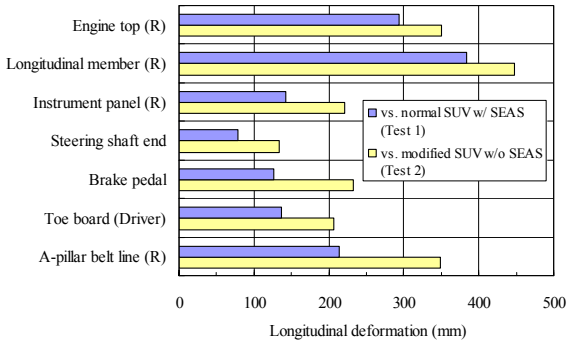

Figure 2. Deformations of small car in Test 1 and Test 2.

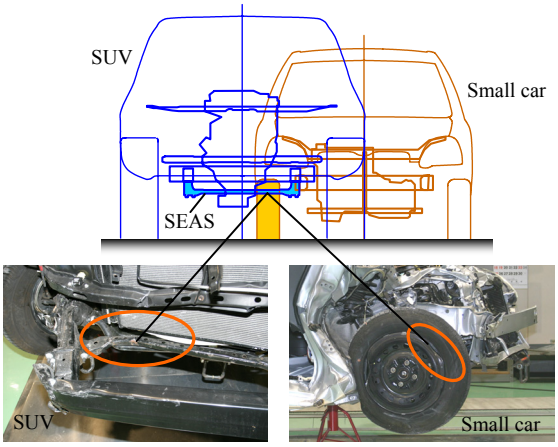

Figure 3. Structure alignment (Test 1).

Figure 4 shows the injury measures of the driver dummy in the small car. In Test 2, the lower extremity injury criteria of the driver dummy, such as femur force, knee displacement and tibia index, exceeded the injury assessment reference values (IARV) due to a greater intrusion. On the other hand in Test 1, the lower extremity injury criteria of the driver dummy were much lower than those in Test 2, although two of the lower extremity injury criteria exceeded their standard values.

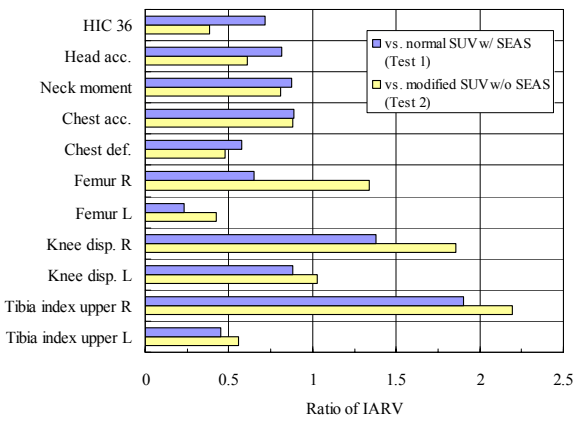

Figure 4. Injury measures of driver dummy in small car in Test 1 and Test 2.

In Test 1, the head injury criterion (HIC) was much higher than that in Test 2 (Figure 4). From a high-speed video, the driver airbag of small car was seen to deploy at 28 ms in the crash into the SUV without SEAS, against 40 ms in the crash into the SUV with the SEAS. In the crash into the SUV with SEAS, it was considered that there was a greater delay in the crash sensor response, which delayed the airbag and seatbelt pretensioner activation and caused higher head acceleration due to contact with the airbag which did not deploy completely and then with the compartment interior. It was guessed that the difference of the crash sensor response between the two tests was caused by the difference of the deformation mode of the longitudinal members.

Full Frontal Crashes

From the SUV-to-car full frontal crash tests (Test 3 and Test 4), it was observed that the normal SUV with a regular longitudinal member height overrode the small car in Test 3 but that the SUV with a lowered longitudinal member height (lowered SUV) did not override the small car in Test 4 as the longitudinal members of the two vehicles interacted effectively. Figure 5 shows the deformations of the small car in the two tests. In Test 3, the small car's longitudinal members deformed upward while its bumper beam intruded and was sheared between the normal SUV's bumper beam and SEAS. In Test 4 with the lowered SUV, the front of the small car exhibited a flat deformation. In the crash into the lowered SUV, the intrusions of the small car's upper components such as the steering wheel and instrument panel were smaller but the intrusion of the toe board was greater than that in the crash into the normal SUV.

The force-deformation characteristics of the small car was compared for the crash into the lowered SUV and for the full-width rigid crash at 55 km/h (Figure 6). To determine the deformation of the car in SUV-to-car crash, it is needed to identify the crash interface. In the lowered SUV-to-car full frontal crash test (Test 4), the crash interface could be determined based on the high speed video from the side view. However, in the normal SUV-to-car test (Test 3), the crash interface could not be determined because the override of the SUV occurred. As shown in Figure 6, the force-deformation characteristics are similar between two tests. Accordingly, when the members of both vehicles in car-to-car crash are in alignment, it is likely that the car deforms similar to the full-width test and the structural behavior can be predicted.

Figure 7 shows the injury measures of the driver dummy in the small car. It was found that the

dummy's right lower extremity generated higher injury measures with the lowered SUV than with the normal SUV but that its left lower extremity generated higher injury measures with the normal SUV. Also, head and neck injury criteria were lower with the lowered SUV than with the normal SUV.

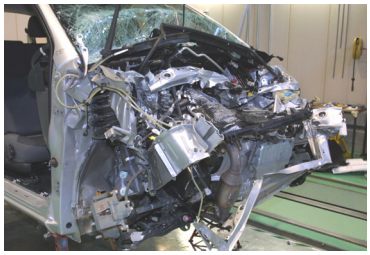

(a) Test 3 (vs. normal SUV w/ SEAS)

(b) Test 4 (vs. lowered SUV w/ SEAS)

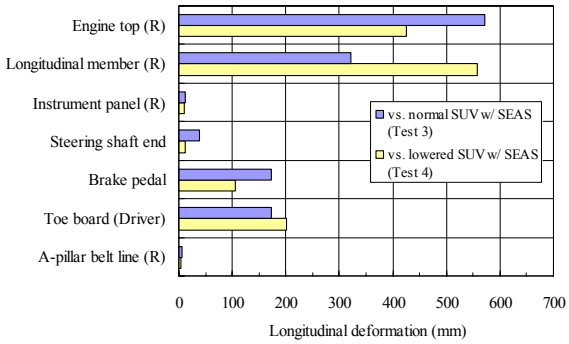

Figure 5. Deformations of the small car in Test 3 and Test 4.

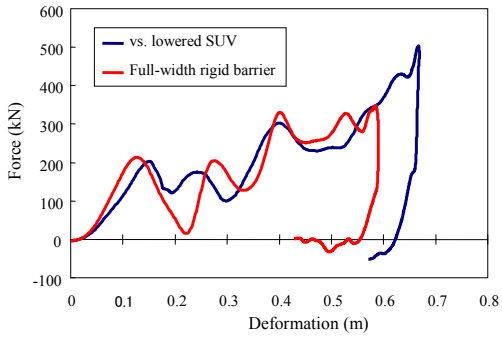

Figure 6. Force-deformation characteristics of small car in crash test into the lowered SUV and in full-width rigid barrier test (55 km/h).

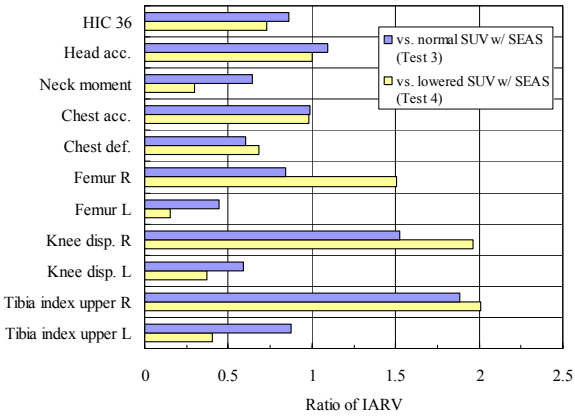

Figure 7. Injury measures of the driver dummy in the small car in Test 3 and Test 4.

Overall, the SUV-to-car full frontal crash tests indicated that structural interaction is an important factor for vehicle compatibility and that an effective means to enhance structural interaction is to improve the geometric alignment of longitudinal member height between vehicles. However, since the injury of the lower legs was increased, this point could be considered to be the problem which it should take notice of.

Although the normal SUV overrode the small car, structural interaction was observed between the SEAS of the normal SUV and the bumper beam of the small car. Assuming the removal of SEAS from the SUV, there may be a more intense overriding of the small car by the SUV. Therefore, it is clear that a SEAS is an important structural component for improving the structural interaction of vehicles.

FULL-WIDTH RIGID AND DEFORMABLE BARRIER TESTS

In order to clarify whether the SEAS can be detected in full-width tests, the barrier force distributions of the normal SUV (with SEAS) and modified SUV (without SEAS) were examined. Table 2 shows the test matrix. Hybrid III test dummies were used for the front seat driver and passenger positions in each vehicle. The barrier force distributions were compared in a full-width deformable barrier (FWDB) test and a full-width rigid barrier (FWRB) test, using 125 x 125 mm high resolution load cells (Figure 8). In the tests, the ground clearance of the load cell barrier was 125 mm, which was different from the 80 mm recommended by IHRA (International Harmonized Research Activities) Phase 1a [1]. The SEAS was aligned with row 2 in the load cell barrier. Thus, the barrier force in row 2 was compared between normal and modified SUVs. The impact velocity was set at 55 km/h. The deformable barrier face used in the FWDB test has two layers [3]. The first layer consists of a 0.34 MPa aluminum honeycomb element, and the second layer consists of a 1.71 MPa element (Figure 9).

Table 2.
Full-width test matrix

Test configuration	Test vehicle	Impact velocity (km/h)	Test mass (kg)
FWDB	Normal SUV w/ SEAS	54.9	2076
FWDB	Modified SUV w/o SEAS	55.0	2076
FWRB	Normal SUV w/ SEAS	54.8	2076

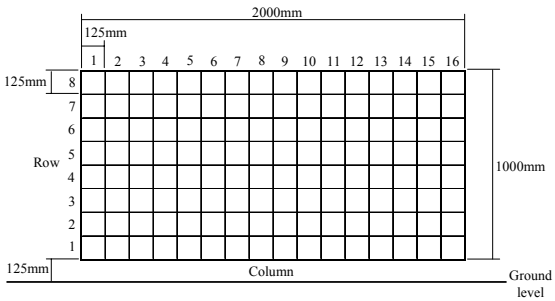

Figure 8. Load cell wall.

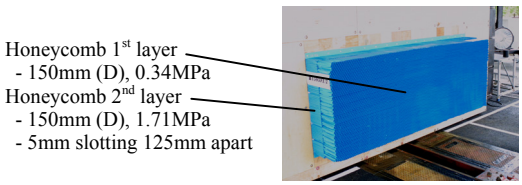

Figure 9. Deformable barrier face.

Figure 10 shows the vehicle deformation of the normal SUV with the SEAS in the FWDB and FWRB tests. In the FWDB test, the SEAS deformed rearward, the front end of the longitudinal members bent downward, and the bumper beam bent backward at its center. In the FWRB test, the front body of the SUV exhibited a flat deformation. The SEAS did not deform rearward in accordance with the axial collapse of the longitudinal members. Thus, SUV deformation differed between deformable and rigid barriers.

Figure 11 shows peak cell force distributions of the SUV with and without the SEAS in the FWDB tests. It was observed that the force on the longitudinal members was extremely large in both vehicles. In the SUV with the SEAS, the front end of its left longitudinal member came into contact with two load cells. The SUV without the SEAS came in contact with three load cells and recorded a high impact force on its engine due to the outward deformation of the left-longitudinal member.

Row 2 with columns from 5 to 12 are the load cells which are in alignment with the SEAS. In row 2 where the SEAS made contact, the row load was 120 kN, against 87 kN in row 2 of the SUV without the SEAS. Comparing Figure 11(a) and (b), it may still be difficult to conclude that the forces of row 2 were generated from the SEAS deformation, because they are spread by the honeycomb. Thus, the force in row 2 was examined according to the vehicle deformation.

(a) with SEAS in FWDB test

(b) with SEAS in FWRB test

Figure 10. Deformations of normal SUV with SEAS in FWDB and FWRB tests.

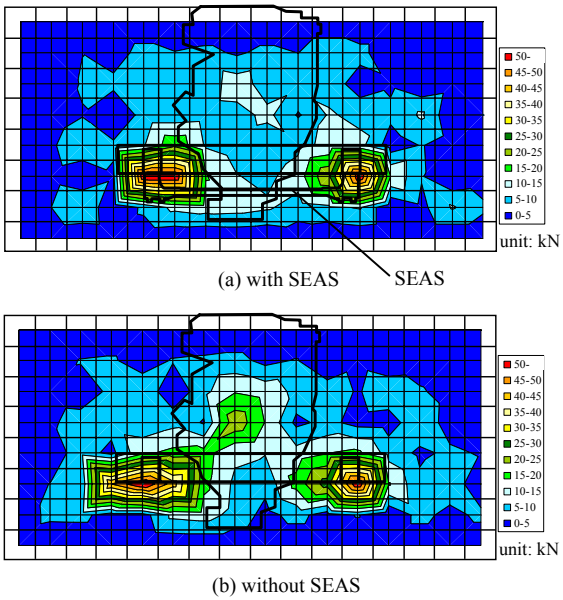

Figure 11. Peak cell force distributions of SUV with and without SEAS in FWDB tests.

The sum of the barrier force in row 2 where SEAS made contact was plotted against the vehicle displacement, which was calculated from a double integral of the passenger compartment acceleration (Figure 12). In the FWDB test, the force increases from the vehicle displacement of 0.4 m, where the SEAS began to contact the barrier. In the SUV without the SEAS, the force level was small in the initial stage, and increased after 0.5 m where the lateral suspension structures started to contact the barrier. Thus, it was demonstrated that the barrier force in row 2 shows the SEAS reaction force in the FWDB test. The result of SUV (with SEAS) in a FWRB test is also shown in Figure 12. The force in row 2 does not increase until the deformation of 0.5 m. Since the vehicle deformation was flat in the FWRB test, the SEAS did not deform rearward and did not generate the reaction force against the rigid barrier. Thus, it will be difficult to measure a SEAS reaction force in FWRB tests.

SEAS detection was examined using the criteria of structural interaction such as average height of force (AHOF) and vertical structural interaction (VSI). The AHOF is a measure of the average height from the ground that a vehicle applies force to the load cell wall, and the intent is to promote structural interaction between vehicles by aligning their stiffest members in the vertical direction [5]. The aim of the VSI is to encourage sufficient vehicle structure in alignment with a common interaction zone, i.e. rows 2 to 5.

Height of force (HOF) was plotted with vehicle displacement (Figure 13), and was almost constant after the bumper beam had come into contact with the barrier because the SUV had a simple frame-type longitudinal member. The AHOF, which was calculated from displacement up to 400 mm (AHOF400), was 551 mm for the SUV with the SEAS, and it increased to 567 mm for the SUV without the SEAS. However, it can not be concluded that the AHOF400 decreased by the SEAS reaction force due to its small force. The engine impact force of the SUV without the SEAS was large as indicated by the collapse of the left-longitudinal member, and it may be more reasonable to consider that a number of factors including engine impact affected the HOF.

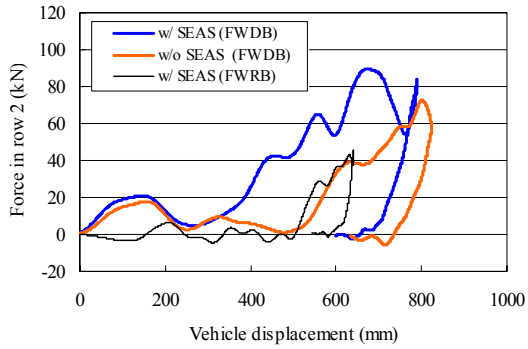

Figure 12. Barrier force in row 2 vs. vehicle displacement for SUV with and without SEAS in FWDB and FWRB tests

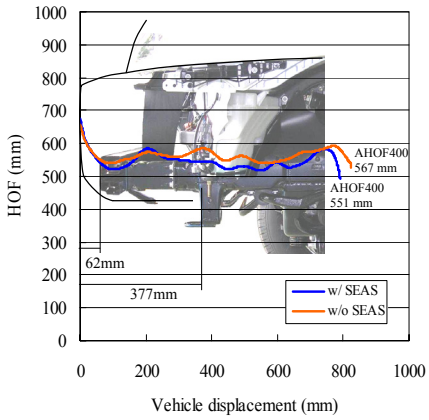

Figure 13. HOF-displacement curves in FWDB tests of SUV with and without SEAS.

Figure 14 shows the peak row load (based on sum of peak load cell forces up to 40 ms) for rows 2 to 5 in the FWDB tests. In row 2 where the SEAS made contact, the row load was 71 kN, against 27 kN in row 2 of the SUV without the SEAS. According to VSI proposed by the Transport Research Laboratory (TRL), which defines rows 2 to 5 as the assessment area, the score was 1.3 for the SUV with the SEAS and 2.0 for the SUV without SEAS. As a result of the FWDB test, it was demonstrated that the SUV with the SEAS is better than the SUV without the SEAS as a structural interaction evaluation. Thus, the VSI will be a useful criterion for assessing the reaction force of SEAS.

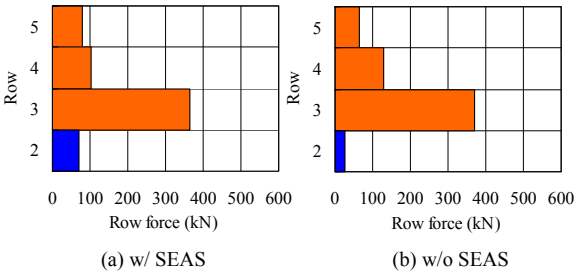

(a) w/ SEAS (b) w/o SEAS

Figure 14. Peak row load in FWDB tests of SUV with and without SEAS.

REPEATABILITY ASSESSMENT OF THE FULL-WIDTH DEFORMABLE TEST

In order to assess the repeatability of the FWDB test, two identical FWDB tests were conducted and vehicle deformations, dummy responses and barrier force distributions were compared between the two tests. In the tests, the ground clearance of the load cell barrier was 80 mm. Table 3 shows the test matrix, using a SUV (with SEAS). Hybrid III test dummies were used for the front seat driver and passenger positions in each vehicle. The impact velocity was 54.9 km/h in the first test (Test 1) and 54.8 km/h in the second test (Test 2). Differences of target location on the barrier were 2 mm left in horizontal direction and 0 mm in vertical direction in Test 1, and 13 mm right in horizontal direction and 0 mm in vertical direction in Test 2.

Table 3.
FWDB test matrix

Test configuration	Test vehicle	Impact velocity (km/h)	Test mass (kg)	Impact accuracy
FWDB (Test 1)	SUV (w/ SEAS)	54.9	2076	2mm left 0mm vertical
FWDB (Test 2)		54.8		13mm right 0mm vertical

Barrier deformations after tests are shown in Figure 15. The honeycomb block deformations caused by the SUV's bumper beam of the SUV substantially differed between the two tests. In the case of Test 1, honeycomb blocks which contacted with the bumper beam were completely deformed. However, in Test 2, the second layer of honeycomb blocks were hardly deformed. They dropped during crashes, and the bumper beam contacted to the back plate directly.

Figure 16 shows the vehicle deformations in the two tests. The vehicle deformations were almost the same in Test 1 and Test 2. However, there was a difference in the deformation mode of the bumper beam between two tests. While the bumper beam bent in Test 1, there was no such bending in Test 2. This difference was considered to be caused by the difference of barrier deformation.

The injury measures of the driver and front passenger dummies are presented in Figure 17. As shown in Figure 17, there were no large differences for injury measures between two tests. The maximum difference was 11.4% for the right upper tibia force of the front passenger, and the difference was less than 5% for many other body parts.

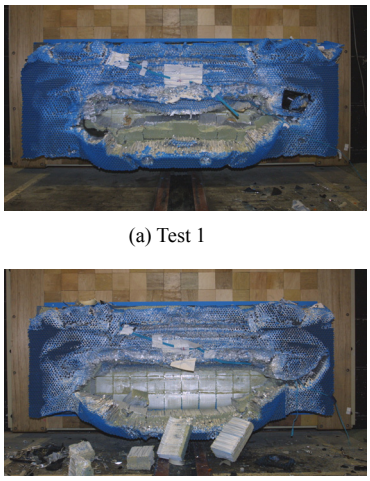

(a) Test 1

(b) Test 2

Figure 15. Barrier deformations.

(a) Test 1

(b) Test 2

Figure 16. Vehicle deformations.

The barrier force-time history is shown in Figure 18. The force curve was almost the same in Test 1 and Test 2, and the maximum force was 657 kN for Test 1 and 672 kN for Test 2. However, the force about 40 ms was greater in Test 2 than in Test 1. In Test 2, since the second layer of honeycomb blocks dropped during crashes, the force generated by the contact with the front end of longitudinal members became great.

Several criteria of structural interaction such as AHOF were compared between two tests. Figure 19 shows HOF-vehicle displacement curve. HOF was almost the same in Test 1 and Test 2. AHOF400 was 546 mm for Test 1 and 555 mm for Test 2, and the difference was small as 9 mm.

The VSI and horizontal structural interaction (HSI) in the assessment area for rows 2 to 5 are shown in Figure 20. The aim of the HSI is to encourage strong crossbeams to adequately distribute rail load and wider structures for lower overlap impacts. As shown in Figure 20, the VSI score was almost the same in Test 1 and Test 2. As for HSI, the outer support measure was equivalent between the two tests. However, the center support measures of the HSI clearly differed between 5.0 for Test 1 and 11.3 for Test 2. The reason for this is that the distributions of the peak cell forces in row 3 are greatly different between the two tests. In Test 2, due to the high force of the longitudinal members, target cell load level was set higher than that in Test 1, while the forces of the 4 cells in the assessment area for the center support were small as a whole compared to Test 1 (Figure 21). These differences were considered to be caused by the difference of barrier deformation.

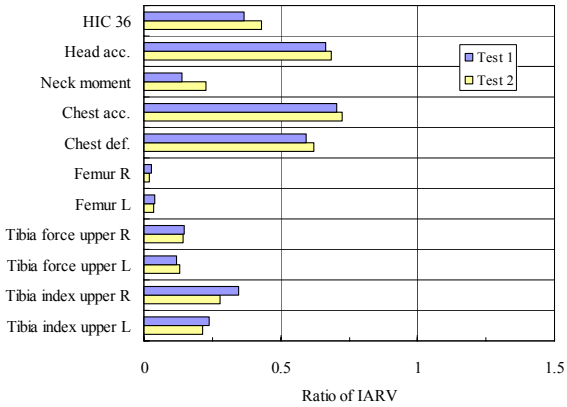

(a) Driver

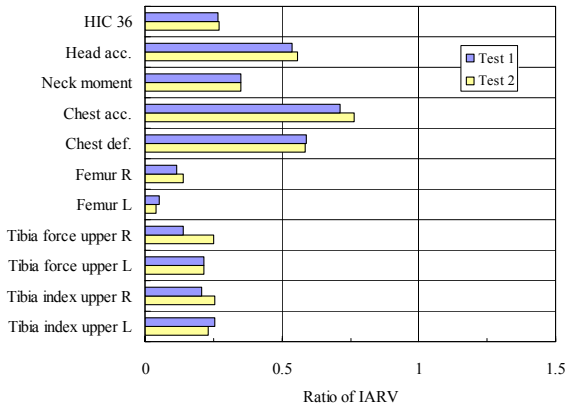

(b) Front passenger

Figure 17. Injury measures of driver and front passenger dummies.

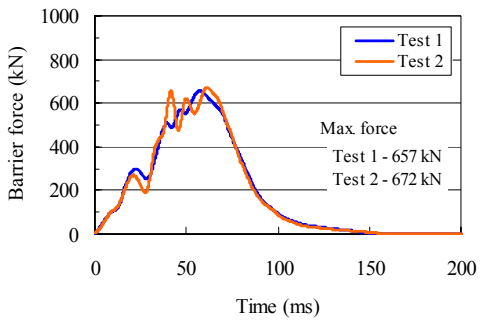

Figure 18. Barrier force-time histories.

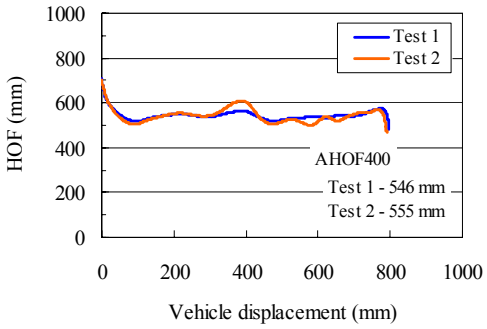

Figure 19. HOF-displacement curves.

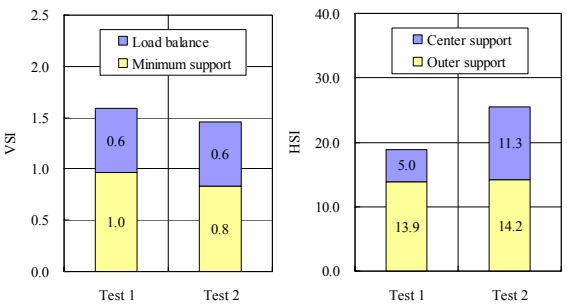

(a) VSI (rows 2 to 5) (b) HSI (rows 2 to 5)

Figure 20. VSI and HSI (rows 2 to 5).

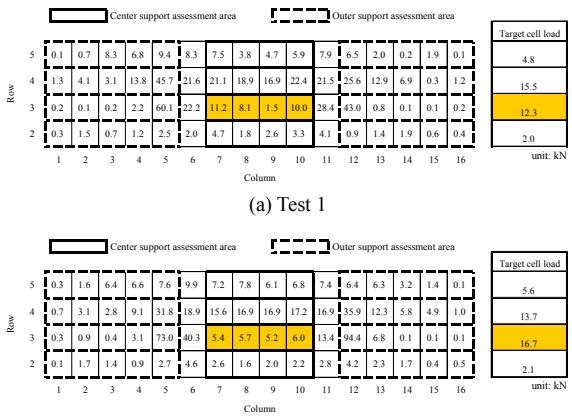

(a) Test 1

(b) Test 2

Figure 21. Peak cell force (up to 40 ms).

CONCLUSIONS

For the improvement and assessment of structural interaction in vehicle-to-vehicle frontal collisions, a series of crash tests using SUVs was conducted. The results are summarized as follows:

1. In SUV-to-small car crash tests, structural interaction was improved by equipping the SUV with a SEAS or by aligning the height of the SUV's longitudinal members with the height of the small car's longitudinal members.

2. SEAS reaction force was detected in a full-width deformable barrier test, and it was demonstrated that VSI will be a useful criterion for assessing structural interaction including SEAS reaction force.

3. Full-width deformable barrier tests indicated a generally good repeatability with regard to dummy responses and vehicle deformations. As compatibility assessment criteria, AHOF and VSI, which are parameters for vertical structural interaction, exhibited good repeatability. However, HSI results were not good due to the difference of barrier deformation.

ACKNOWLEDGEMENT

The authors gratefully acknowledge JAMA for providing crash test data.

REFERENCES

[1] O'Reilly, P., "Status Report of IHRA Compatibility Working Group," 19th International Conference on the Enhanced Safety of Vehicles, Paper No. 365, 2005

[2] Edwards, M., et al., "The Essential Requirements for Compatible Cars in Frontal Collisions," 17th International Conference on the Enhanced Safety of Vehicles, Paper No. 158, 2001

[3] Edwards, M., et al., "Development of Test Procedures and Performance Criteria to improve Compatibility in Car Frontal Collisions," 18th International Conference on the Enhanced Safety of Vehicles, Paper No. 86, 2003

[4] Hollowell, W.T., et al., "NHTSA's research program for vehicle aggressivity and compatibility," ImechE Conference, 2002

[5] Summers, S., et al., "Design Considerations for a Compatibility Test Procedure," Society of Automotive Engineers, Paper No. 2002-01-1022, 2002